



**ZRC SAZU**



Univerza v Ljubljani  
Fakulteta za gradbeništvo  
in geodezijo



**GOZDARSKI INŠTITUT SLOVENIJE**  
SLOVENIAN FORESTRY INSTITUTE

# Land surface phenology from satellite data<sup>1</sup>

## Technical report

version 1

Urša Kanjir<sup>a</sup>, Ana Potočnik Buhvald<sup>b</sup>, Mitja Skudnik<sup>c</sup>, Liza Stančič<sup>a</sup>, Krištof Oštir<sup>b</sup>

<sup>a</sup> Research Centre of the Slovenian Academy of Sciences and Arts

<sup>b</sup> University of Ljubljana, Faculty of Civil and Geodetic Engineering

<sup>c</sup> Slovenian Forestry Institute

December 2022

<sup>1</sup> This study was funded by the Slovenian Research Agency research project No. J2-3055. The view expressed herein can in no way be taken to reflect the official opinion of the financier.

© ZRC SAZU [2022]. The copyright in this document is vested in ZRC SAZU. This document may only be reproduced in whole or in part, or stored in a retrieval system, or transmitted in any form, or by any means electronic, mechanical, photocopying or otherwise, either with the prior permission of ZRC SAZU.

# Land surface phenology from satellite data

Technical Report, version 1

## Contributing authors in alphabetical order:

Urša Kanjir\*

Ana Potočnik Buhvald

Mitja Skudnik

Liza Stančič

Krištof Oštir

## \*Corresponding author

**Urša Kanjir**

Research Centre of the Slovenian Academy of Sciences and Arts

Novi trg 2

SI-1000 Ljubljana

Slovenia

e: [ursa.kanjir@zrc-sazu.si](mailto:ursa.kanjir@zrc-sazu.si)

## Abstract

This technical report describes the analysis of land surface phenology through the use of space-borne optical sensors focusing on different forest types in different regions of Slovenia. Specifically, the objective of this study was to investigate the reliability of MODIS and Sentinel-2 satellite imagery for determining key phenological phases of different forest types in comparison with different types of field measurements, and to compare different algorithms for determining phenological phases from vegetation indices. In addition, we tested which spectral channels of Sentinel-2 imagery and vegetation indices provide the best detection of phenological phases, how they depend on each other, and how accurately they can identify key phenological phases of the multi-year growth cycles, especially of European beech (*Fagus sylvatica*).

## Izvleček

Tehnično poročilo opisuje analizo fenologije zemeljskega površja z uporabo satelitskih optičnih senzorjev, s fokusom na različnih tipih gozdov v različnih regijah Slovenije. Natančneje, namen te študije je bilo preučiti zanesljivost satelitskih posnetkov MODIS in Sentinel-2 za določevanje ključnih fenoloških faz različnih tipov gozdov v primerjavi z različnimi vrstami terenskih meritev in primerjati različne algoritme za določanje fenoloških faz iz vegetacijskih indeksov. Poleg tega smo preverili, kateri spektralni kanali Sentinel-2 posnetkov in vegetacijski indeksi omogočajo najboljše določanje fenoloških faz, kako so odvisni drug od drugega in kako natančno lahko določijo ključne fenološke faze večletnih rastnih ciklov, zlasti evropske bukve (*Fagus sylvatica*).

# Contents

1	Introduction	6
2	Data used	9
2.1	Satellite data	9
2.1.1	MODIS	9
2.1.2	SENTINEL-2	10
2.2	In-situ data	11
2.2.1	ARSO phenological data	11
2.2.2	GIS ICP Forest phenological data	11
2.2.3	ARSO meteorological data	12
2.3	Additional data	12
3	Study areas	13
4	Methods for obtaining phenological phases	16
4.1	Extracting phenology from MODIS data	16
4.1.1	Seasonal midpoint method	16
4.1.2	TIMESAT, version 3.3	17
4.2	Extracting phenology from Sentinel-2 data	18
4.2.1	Selection of key information for phenology monitoring from Sentinel-2 data	18
4.2.2	DATimeS, version 1.10	20
5	Overview of results	22
5.1	Linking meteorological data with Sentinel-2 time series and selection of products illustrating phenology	22
5.2	Detection of phenological phases from Sentinel-2 data	24
5.3	Comparison of field data with MODIS-derived phenological phases	27
5.4	Comparison of the different approaches for the detection of phenological phases	30
6	Conclusion	32
7	References	34

# 1 Introduction

The first phenological records date back to about 3000 years ago in China, and in Japan the phenomenon of cherry blossom has been recorded for 1200 years. Phenology as a science began to develop in the mid-18th century, when several records of phenological data appeared. Swedish botanist Carl Linne was the first to describe the methods used to create phenological calendars in his *Philosophia Botanica*, relating phenological phases (leaf unfolding, flowering, yellowing, and leaf fall) to weather and climate factors. Linne also founded the first phenological network in what is now Sweden and Finland. At the end of the 19th century, systematic phenological observations began on European soil and the first phenological maps were produced. With the establishment of a number of national phenological observation networks in Europe in the mid-20th century, the so-called modern era of phenology began. Most of them were created within the framework of national meteorological services. In 1953, the Commission for Agrometeorology of the World Meteorological Organisation (WMO) recommended its members to conduct regular meteorological observations. In 1993, the Global Phenological Monitoring (GPM) was established to expand the network of phenological observations worldwide. In 2001, the European Phenological Network was established to collect phenological data from international, national, regional, and local phenological networks in Europe and America. Its main task is to enhance phenological measurements collected over several decades to study the effects of global climate change on flora and fauna and possible adaptations (Žust et al., 2016).

The Slovenian National Phenological Network was founded in 1951. Since 2001, phenological observations have been part of the regular activities of the Department of Agrometeorology at the Environmental Agency of the Republic of Slovenia (ARSO). Initially, observations were collected at 30 phenological stations, later the number of stations exceeded 200, and today there are still just over 40 active stations, evenly distributed, but still barely meeting the requirements for sufficient coverage of Slovenia's topographically diverse and rugged terrain (Žust et al., 2016).

At phenological stations, the observer visually records the date of occurrence of phenological phases such as leaf growth, first budding, flowering, fall yellowing, and leaf fall in various plant species. More recently the observer has been replaced at some sites by permanently installed digital cameras that can monitor vegetation on a daily basis. The photos thus represent continuous observations that allow us to identify phenological phases based on the difference in relative reflectance in the red, green, and blue channels while performing even more similar phenological analyses (Vrieling et al., 2018). Over the past decade, with the development of space technologies, satellite sensors have often replaced images from fixed digital cameras in phenological studies.

Remote sensing data offer great potential for monitoring vegetation dynamics, especially over large areas. Such data provide temporally repeated observations that allow a better understanding of the temporal and spatial dynamics of ecosystems (Sjöström et al., 2011). Most analyses of vegetation phenology using remote sensing techniques focus on plant chlorophyll content and can therefore be studied using seasonal changes in spectral and biophysical indices. Such analyses are used to determine the state of plant cover, from which various stress conditions (diseases, drought, sleet ) can be inferred, in agriculture for crop production planning and for planning agricultural interventions or for monitoring changes in biodiversity (Žust et al., 2016). They also show variability as a result of land-use change, climate change, or other changes (Eklundh and Jönsson, 2017). The description of growing seasons as part of vegetation phenology mainly involves the definition of phenological phases (or matrices or parameters), such as the beginning and end of the growing season. Phenological phases depend on the

type of vegetation observed, climatic location, air temperature, precipitation, duration of solar radiation, etc.

Several authors have addressed the determination of phenological phases from optical satellite imagery (Eklundh and Jönsson, 2017; Garonna et al., 2016; Vrieling et al., 2018; Wessels et al., 2011; Zhang et al., 2003). Each satellite sensor has a unique combination of spatial and temporal resolution. The most commonly used sensors for plant phenology observations are Landsat, Sentinel-2, and MODIS (Bolton et al., 2020; Younes et al., 2021). Phenology detection from satellite data depends not only on the sensor, but also on the amount of data available for the study and the environmental factors in the image (e.g., cloud cover). Some studies address plant phenology using one year of data (Kowalski et al., 2020), others examine the alleged phenology over decades (Garonna et al., 2016; Melaas et al., 2018). The amounts of data depend on the sensor being used, and successive acquisitions of images over an extended period of time are referred to as time series.

Accurate time series are essential for monitoring and studying vegetation and its changes during the growing season. The dynamics of vegetation or the developmental phase of phenology is time-dependent and is reflected in the time series of satellite imagery or its vegetation indices by changing values that increase in spring, peak in summer, and then decrease in early fall (Figure 1).

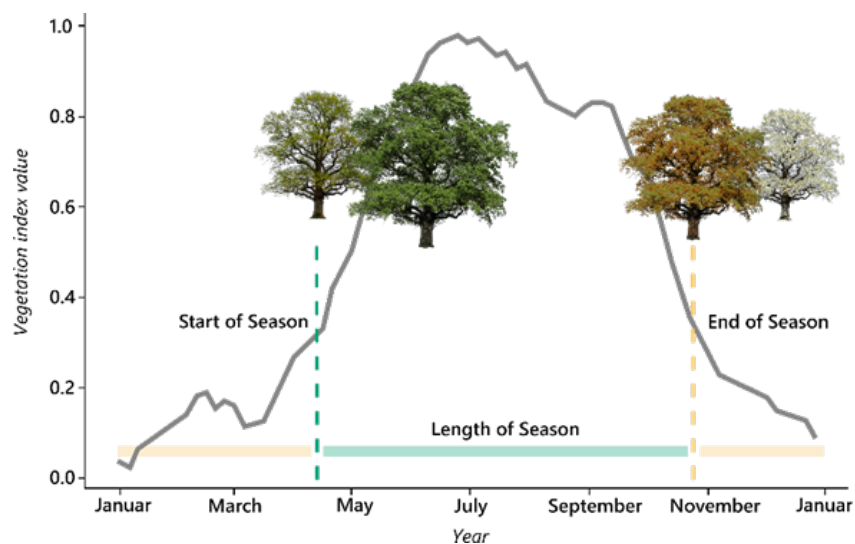


Figure 1. The main phenological phases in the growing season and the values of the vegetation index during the year.

To achieve good results, time series data from satellite imagery should be as consistent as possible or occur in as similar a temporal sequence as possible. The denser the satellite data, the more accurately the phenological phases can be determined. The satellite imagery that makes up the time series is often affected by atmospheric noise, so it is highly recommended for phenological studies to smooth or generalise the time series prior to analysis. A number of smoothing techniques are available to correct and smooth time series data and to aid in the estimation of phenological phases.

The objective of this study was to investigate the reliability of MODIS and Sentinel-2 satellite imagery for determining important phenological phases of different forest types compared to different types of field measurements, and to compare different algorithms for determining phenological phases from vegetation indices. In addition, we tested which spectral channels of Sentinel-2 imagery and vegetation indices provide the best detection of phenological phases, how they depend on each other, and how

accurately they can identify key phenological phases of the multi-year growth cycles, especially of European beech (*Fagus sylvatica*).

## 2 Data used

The data used for the analysis can be broadly divided into two classes: modelled data represented by satellite imagery and measured or field (in-situ) data. We also add other data to the overview, with most data coming from meteorological stations.

Satellite data can be used to observe the phenology of individual plants, but these estimates are always more general than direct field observations, which are usually limited to small areas and short observation periods.

### 2.1 Satellite data

Different satellite sensors have different spatial resolutions, which determine the unit or size of the observation area. Low or medium spatial resolution imagery, such as MODIS with spatial resolution from 250 m to 8 km and temporal resolution of one day, allows us to monitor phenology at global, national, and regional scales. This allows us to monitor plant communities, provided they are not growing in too many heterogeneous areas. The medium spatial resolution data usually do not reflect the actual phenological variability, nor can they be used to analyse individual plant species (Melaas et al., 2013; Vrieling et al., 2018). High spatial resolution imagery, such as Sentinel-1 and Sentinel-2, has great potential for detecting phenological phenomena also at the local or plot level. The following sections present the usefulness of MODIS and Sentinel-2 systems for phenology detection and analysis.

#### 2.1.1 MODIS

In this study, we used MODIS (Moderate Resolution Imaging Spectroradiometer) images on board the Terra and Aqua satellites (NASA) to estimate vegetative phenological phases. MODIS observes the Earth in the visible and infrared range of the electromagnetic spectrum with 250 m spatial resolution, offering a long and dense time series. Thanks to its regular acquisitions (every two days, composites of every 8 days) and good atmospheric corrections, it provides suitable data for vegetation studies (Zhang et al., 2003).

In our case, we used MODIS imagery, or the collection of NDVI products from 2000 up to and including 2018, which resulted in a total of 812 usable NDVI images for the whole of Slovenia. The NDVI vegetation index is produced by the contractor as a 16-day average product of the two satellites' images with multiple spatial resolutions. NDVI was chosen for the analysis because it represents a strong correlation with green biomass and is often used to observe vegetation from remotely sensed data (Tucker, 1979). NDVI uses reflected radiation in the near-infrared and visible red wavelengths to quantify the density of vegetation cover. It is expressed as:

$$NDVI = \frac{\text{near IR band} - \text{red band}}{\text{near IR band} + \text{red band}}$$

NDVI values range between -1 and 1, with higher values indicating greater photosynthetic activity.

Clouds and poor atmospheric conditions tend to lower NDVI values (Chen et al., 2004) and cause sudden drops in the time series, which are treated as noise and need to be removed from the time series by smoothing procedures (Pettorelli et al., 2005). It is common practise to use mathematical functions to smooth the time series curve of satellite imagery to obtain continuous data useful for phenology modelling (Noumonvi et al., 2021). Cai et al. (2017) tested several time series smoothing methods (e.g.,

Savitzky-Golay method, locally weighted regression smoothing, spline smoothing, asymmetric Gaussian smoothing, double logistic function fitting) on MODIS NDVI time series and found that all methods reduce noise in the images and improve the quality of the observations, but no method always performs better than the others. Each method has its advantages and disadvantages, and the choice of model depends on the purpose of the study.

## 2.1.2 SENTINEL-2

Sentinel-2 multispectral optical satellite imagery has been available for the same area every 5 days since March 2017. The spatial resolution of the visible and infrared spectral bands used for Sentinel-2 is 10 m (channels B02, B03, B04, B08), 20 m (bands B05, B06, B07, B8A, B11, B12), and 60 m (bands B01, B09, B10). The major limitation in their use, similar to MODIS data, is the presence of atmospheric noise (clouds, haze, etc.). This increases the uncertainty in determining phenological phases when monitoring phenology.

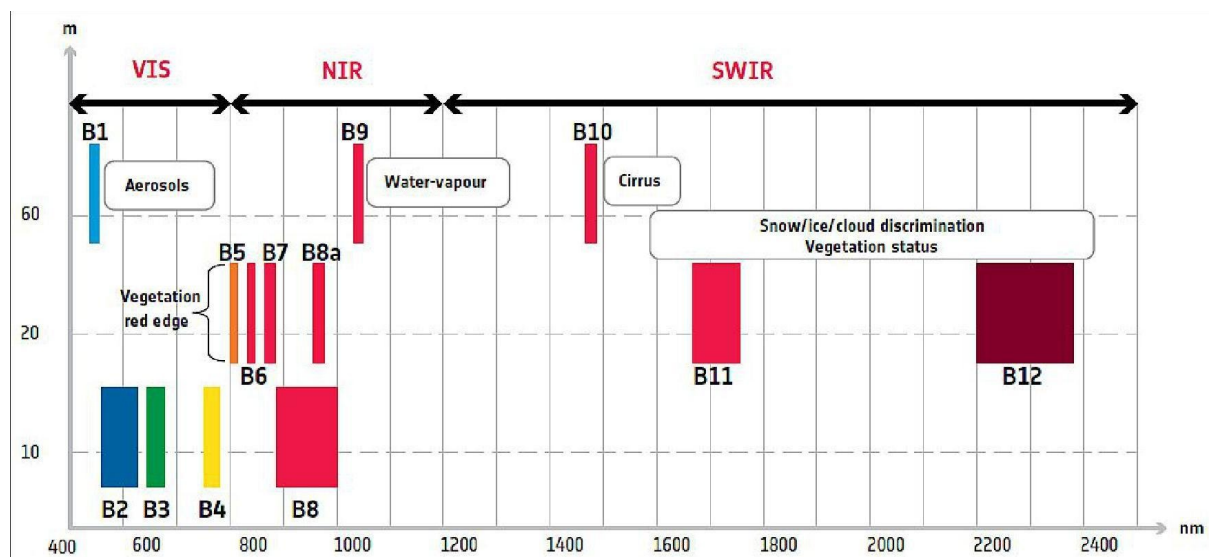


Figure 2. Spectral characteristics of Sentinel 2

In our case, we downloaded and used all existing Sentinel-2 data (spectral band reflectance and cloud cover (%)) from 2017 to 2022, using the eo-learn library and the statistical API from the Sentinel-HUB platform. From these, we built dense time series (areas where the orbits of the Sentinel-2 satellites overlap are denser than 3 days) and added 22 vegetation indices (Table 1). The vegetation indices analysed were taken from various studies dealing with satellite imagery and phenology. They represent spectral transformations that combine two or more spectral bands and show different vegetation properties or biophysical parameters (e.g. pigment, water content, chlorophyll or vegetation structure) that can be used to objectively monitor vegetation dynamics on a regional or even global scale.

Table 1. Overview of the vegetation indices used in the study.

Index	Formula (Sentinel-2)	Reference
NDVI	$(B08 - B04) / (B08 + B04)$ ;	Tucker, 1979
TNDVI	$\sqrt{(B08 - B04) / (B08 + B04)} + 0.5$ ;	Akkartala et al., 2004
GNDVI2	$(B07 - B03) / (B07 + B03)$ ;	Lymburner et al., 2000
PSSRa	$B07 / B04$	Blackburn, 1998
RVI	$B08 / B04$	Pearson and Miller, 1972

Index	Formula (Sentinel-2)	Reference
<b>ARVI</b>	$(B8A - B04 - y * (B04 - B02)) / (B8A + B04 - y * (B04 - B02)); y = 0.106$	Tanre et al., 1992
<b>BWDRVI</b>	$(0.1 * B07 - B02) / (0.1 * B07 + B02)$	Sonobe et al., 2018
<b>SAVI</b>	$(B08 - B04) / (B08 + B04 + L) * (1.0 + L); L = 0.428$	Huete, 1988
<b>EVI2</b>	$2.5 * (B08 - B04) / (1 + B08 + 2.4 * B04);$	Huete et al., 2011
<b>EVI</b>	$2.5 * (B08 - B04) / ((B08 + 6.0 * B04 - 7.5 * B02) + 1.0);$	Huete, 1997
<b>DSWI</b>	$(B08 - B03) / (B11 + B04)$	Hościło, 2016
<b>GCI</b>	$(B08 / B03) - 1;$	EOS Data Analytics, 2022
<b>GNDVI</b>	$(B08 - B03) / (B08 + B03);$	Gitelson et al., 1996
<b>IRECI</b>	$(B07 - B04) / (B05 / B06)$	Frampton et al., 2013
<b>NDI45</b>	$(B05 - B04) / (B05 + B04)$	Delegido et al., 2011
<b>SIPI</b>	$(B08 - B01) / (B08 - B04);$	EOS Data Analytics, 2022
<b>NBR</b>	$(B08 - B12) / (B8 + B12);$	García and Caselles, 1991
<b>MCARI</b>	$((B05 - B04) - 0.2 * (B05 - B03)) * (B05 / B04);$	Daughtry et al., 2000
<b>RGVI</b>	$B03 - B04 / B03 + B04) + 0.5$	Löw and Koukal, 2020
<b>BNIR</b>	$B08 / 5500$	Löw and Koukal, 2020
<b>NDI45</b>	$(B05 - B04) / (B05 + B04);$	Delegido et al., 2011
<b>S2REP</b>	$705 + 35 * ((B04 + B07) / 2 - B05) / (B06 - B05)$	Frampton et al., 2013
<b>NDMI</b>	$(B08 - B11) / (B08 + B11);$	Gao, 1996

## 2.2 In-situ data

The field data used in this work were used to verify the phenological parameters obtained from the satellite images. It is important to note that different authors define phenological seasonal phases differently. The reference data used, either collected in the field or calculated from ground measurements, are listed in the following subsections.

### 2.2.1 ARSO phenological data

Source: ARSO Phenological Data Archive

Because different phases of phenological development are measured for different plant species, we selected data from linden (*Tilia platyphyllos*) for comparison with MODIS data, and beech (*Fagus sylvatica*) for comparison with Sentinel-2 data. For linden, we used data at the time of first leaf emergence (when a few fully open and erect leaves appear on the observed tree, the leaves have the characteristic shape of the species but are not yet the final size), at the time of general yellowing, and at the time of general leaf drop (when more than half of the leaves on the observed tree have autumnally yellowed or dropped). For beech, we paid attention to the appearance of the first leaves (when 10% of the leaves on the tree have a final shape but not yet a final size or colour) and general leaf yellowing (when 50% of the leaves on the tree change colour from green to yellow, red, or brown).

It is important to note that the data for each tree may vary depending on the actual location. Generally, a tree is located within 1 km, or more in exceptional cases, of the coordinates given.

### 2.2.2 GIS ICP Forest phenological data

Source: Slovenian forest institute

These phenological data were collected on trees in ICP Forests Level II plots in Slovenia. The II level plots were established in some selected forest types that are of national greater importance. The ICP Forests programme (International Co-operative Programme on the Assessment and Monitoring of Air Pollution

Effects on Forests") was initiated in 1985 by the United Nations Economic Commission for Europe on the basis of the Convention on Long-Range Transboundary Air Pollution (CLRTAP). In Slovenia, the programme began in 1978 (Level I plots), but was not regulated until 2000 with the adoption of the Forest Protection Regulation. Level II plots, where phenological observations are also carried out, were established in 2003.

Phenological data were collected for different forest tree species, including beech (*Fagus sylvatica*), oak (*Quercus robur*) and hornbeam (*Carpinus betulus*). According to the internationally harmonised ICP Forests methodology (Raspe et al., 2020) means the beginning of the phenological growing season of forests, when most of the first leaves of a tree open in the spring, and the end, when most of the leaves change colour in the fall. Each phenological phase (foliage, coloration, and leaf fall) is rated on a five-point scale (< 1%, 1-33%, 34-66%, 67-99%, > 99%).

### 2.2.3 ARSO meteorological data

Source: ARSO National Meteorological Archive

Meteorological data on the beginning and end of the growing season are available for the period beginning in 1991. The meteorological beginning of the growing season is defined by ARSO on the basis of an interval of five degrees Celsius in spring and autumn. This means that the beginning of the season in spring requires at least six consecutive days with an average temperature greater than 5° C, while the end of the growing season in autumn is characterised by six consecutive days with a measured average temperature lower than 5° C. These data were used as an additional observation to test whether satellite imagery, specifically MODIS data, is due to its median spatial resolution more responsive to meteorological than to phenological in-situ data.

For the analysis with the Sentinel-2 data, we also used additional data from the meteorological data archive: daily maximum air temperatures (°C), daily minimum air temperatures (°C), daily average air temperatures (°C), daily average precipitation (mm), sunshine duration (h), snow depth/new snow, and cloud cover (%).

## 2.3 Additional data

In addition to all the data described above, additional data were also used for the study, namely digital elevation model data with a resolution of 25 m (source: GURS) and tree stand data (source: GIS, ZGS).

### 3 Study areas

The study area includes points throughout Slovenia. It should be remembered that most of the plant species considered in this study do not form large-scale pure stands. Due to the spatial variability of the landscape and climatic conditions, different lengths of vegetation periods can be observed, which are reflected in the spatio-temporal pattern of the NDVI. In all cases, only one phenological season is observed in Slovenia. For the MODIS and Sentinel-2 observations, we analysed different sites in Slovenia. The actual locations of these stations do not reflect the exact location of the stations. For example, for meteorological stations whose locations are known, a given coordinate may differ from the actual coordinate by more than 100 metres.

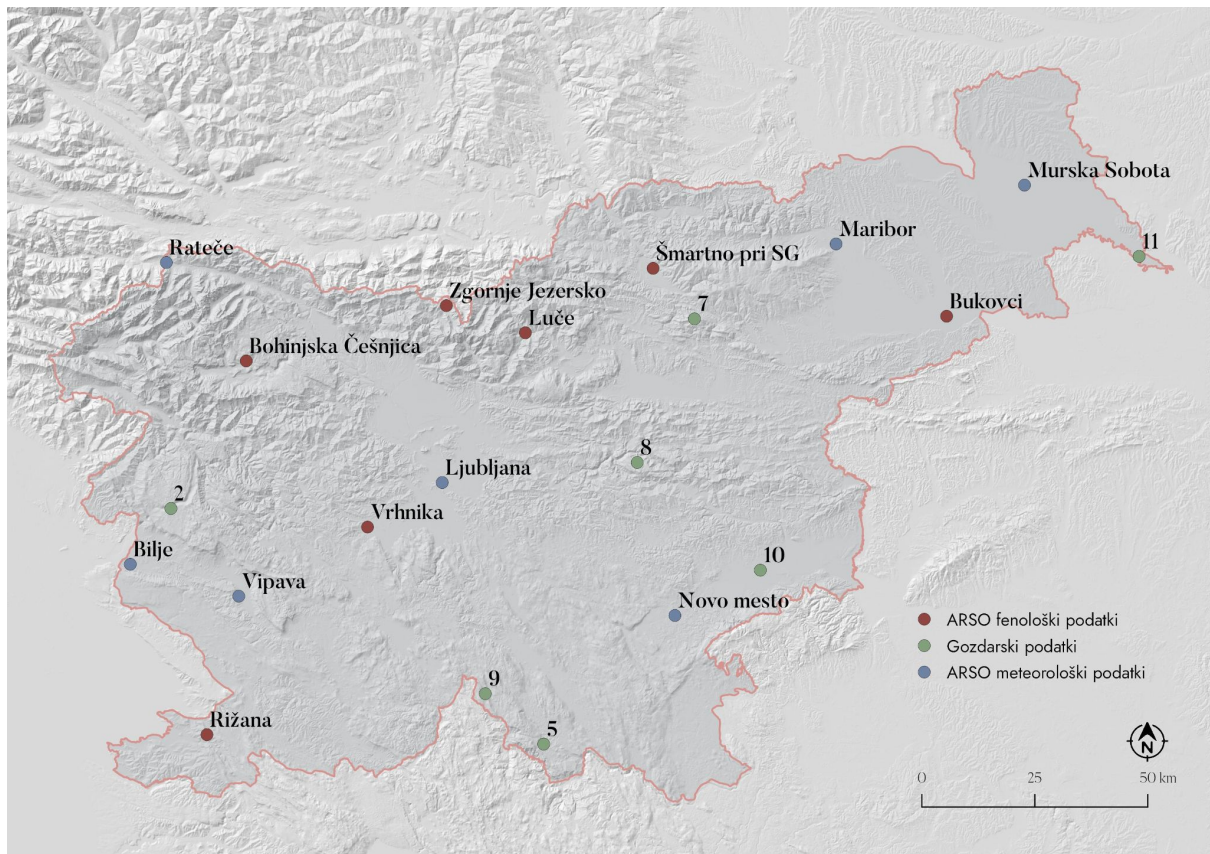


Figure 3. Locations where we tested the usefulness of MODIS satellite imagery for determining phenological phases.

Phenological phases were calculated from the MODIS NDVI time series for a total of 21 points: seven point locations for all three data types (see Figure 3).

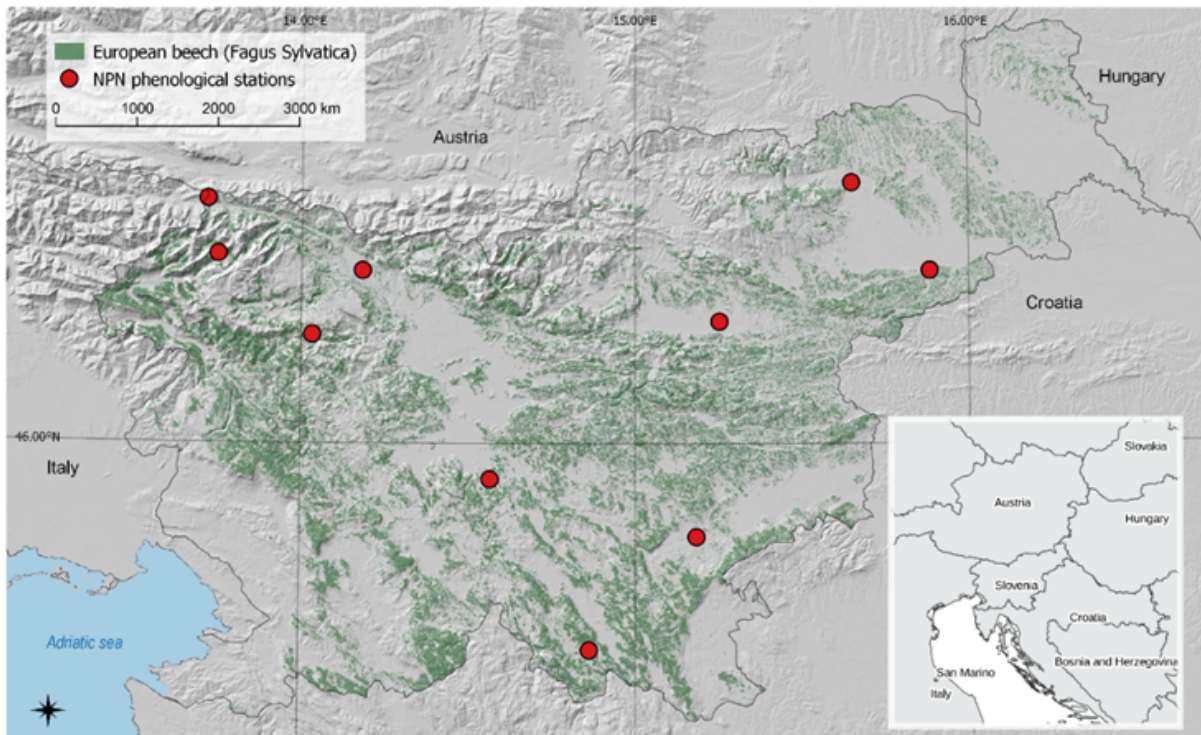


Figure 4. Locations of study areas for phenological monitoring with Sentinel-2 satellite imagery and distribution of beech stands in Slovenia (in green).

The beech observation sites are distributed among different ecological regions (Table 2), thus covering a heterogeneous sample of observations covering the topographically diverse and rugged terrain of Slovenia. The sites are characterised by pure beech stands (the proportion of beech in each stand is more than 90%) of 20 × 20 m size and are located in close proximity to the ARSO monitoring stations. The five monitoring stations were taken from the study "Prediction of plant phenological development on the basis of agrometeorological variables in Slovenia" (Črepinšek, 2002). There, the stations were selected on the basis of two criteria, namely that the selected meteorological station is also a phenological station and that the sample of selected stations covers climatically different parts of Slovenia. In our study, 5 stations were added that are not part of the above study. At all sites we searched for stands with similar meteorological and spatial characteristics as the phenological stations of the National Phenological Network (NPN). Each sample point was manually verified by visual interpretation.

Table 2. Observation sites in study areas with spatial and meteorological characteristics.

ID	GGO Region	Presence of Beech (%)	NPN station	Altitude (station)	Altitude (stand)	Slope (stand)	Aspect (stand)	Num. of available / usable data	Climate Normals (1981-2010)	
									T (°C)	P (mm)
33	2	93	Rateče	864	985	44	SE	366/777	6,6	1459
380	2	99	Lesce	515	524	31	S	182/390	8,7	1418
451	3	92	Sorica	820	826	44	SW	163/390		
696	4	95	Želimlje	310	392	39	NE	177/390		
731	6	95	Novi Lazi	540	543	9	NW	186/390		
768	7	91	Novo mesto	220	222	5	NW	189/389	10,4	1171
789	9	95	Celje	241	317	25	E	188/389	9,8	1113
810	12	92	Podlehnik	320	319	29	N	192/389		
860	12	90	Maribor	275	265	0	SW	185/389	10,6	893
873	1	92	Trenta	622	712	33	SE	364/777		

## 4 Methods for obtaining phenological phases

The choice of method for determining phenological parameters depends on the vegetation index used, the phenological threshold chosen (e.g., what defines the beginning/end of the season), and how that threshold is converted to a vegetation index value or to a value for examining vegetation type (Eklundh and Jönsson, 2017).

### 4.1 Extracting phenology from MODIS data

To accurately determine the growing season and its characteristics using MODIS data for each year, we developed our own approach in the R programming language (for the workflow see Figure 5) and used the TIMESAT tool to compare the results.

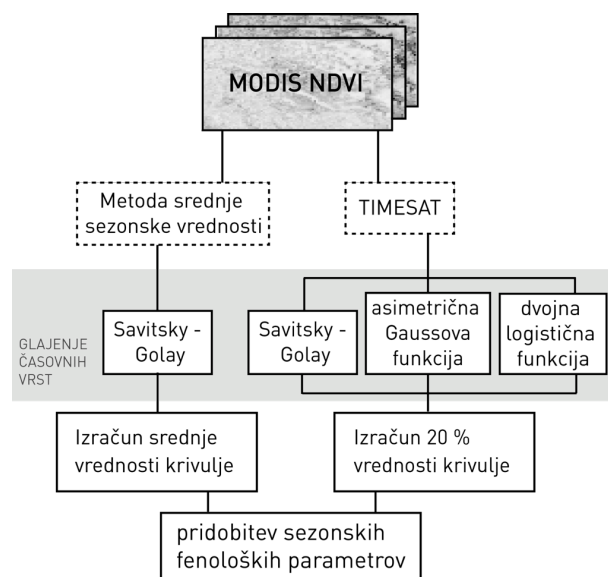


Figure 5. MODIS satellite image processing workflow for defining phenological phases.

#### 4.1.1 Seasonal midpoint method

The approach to determining key phenological phases that we developed for this work in the R software environment works by determining the threshold of the NDVI curve and is relatively simple. To ensure that the data set does not contain additional noise, the time series MODIS NDVI is first smoothed with an adaptive Savitzky-Golay filter (Savitzky and Golay, 1964). This smoothing method is particularly suitable for smoothing NDVI time series because it can remove abnormally high and low values (Chen et al., 2004).

After smoothing the time series for each year, we calculate the peaks (maxima) and valleys (minima) on the temporal histogram of NDVI values. To calculate phenological metrics, a specific threshold or limit is often set to define the beginning or end of the growing season. The beginning of the growing season usually refers to the date when NDVI values increase significantly, while the end marks the time when plant greening indicator values decrease significantly. The most commonly used threshold for their determination is 50% of the amplitude of the vegetation index considered in the given season. This means that the beginning (end) of the growing season is defined as the median or midpoint between the minimum and maximum values on the curve in an ascending (descending) histogram of NDVI values

in a given year (Figure 6), similar to Noumonvi et al. (2021) or Restrepo-Coupe et al. (2015). However, the choice of the median on the curve is a pragmatic decision because, as Noumonvi et al. (2021) note, the best threshold chosen to determine the beginning or end of the growing season may vary depending on the location of the station or the type of vegetation observed. Huang et al. (2019) noted that there is no optimal threshold that is suitable for all plant species.

The seasonal midpoint method can be applied dynamically for each year, but it is very sensitive to snow cover, cloud cover, drought, and similar extremes that can cause large differences in the results. The results obtained are tabulated for each individual year as day of the year (DOY).

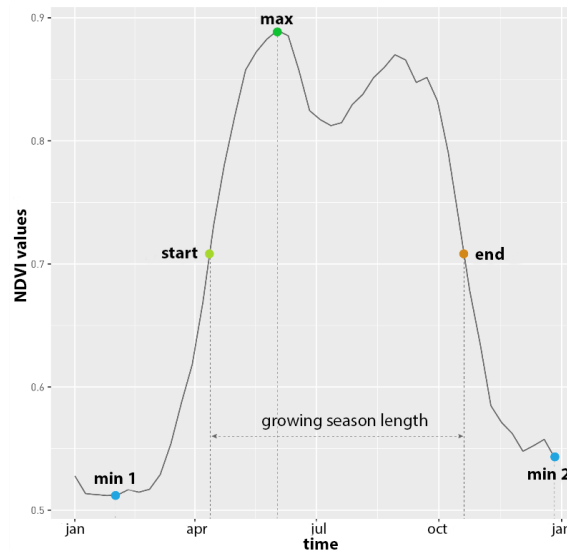


Figure 6. Phenological (seasonal) phases calculated by the seasonal midpoint method based on NDVI values from satellite images.

We further compared the results obtained with the described approach with the different approaches obtained with the TIMESAT tool.

#### 4.1.2 TIMESAT, version 3.3

TIMESAT (Jönsson and Eklundh, 2004) is a widely used software package for determining a large number of phenological phases. It is a computationally simple but robust tool that is widely used in studies that investigate vegetation phenology using time series of satellite imagery (e.g. Cho et al., 2017; Davis et al., 2017; O'Connor et al., 2012; Van Leeuwen, 2008; Wessels et al., 2011). The results come from different data smoothing approaches that influence the definition of the phenological phases (Savitzky-Golay, Assymmetric Gaussian, Double Logistic, Coarse Seasonality). The final choice of method depends on the characteristics of the input data and is decided by testing the fit of the function to the original data. For testing purposes, we tried several different approaches to determine the most appropriate one.

The determination of seasonal phases in TIMESAT is defined in such a way that the beginning of the vegetation period is determined when the values on the curve increase by 20% of the seasonal amplitude and vice versa, and the end of the vegetation period is calculated when the amplitude decreases by 80%. Although there are many other software packages for determining phenological phases (e.g., PhenoSat, QPhenoMetrics, Phenex, Greenbrown), in this study we tested the usefulness of the methods already integrated into TIMESAT.

## 4.2 Extracting phenology from Sentinel-2 data

As can be seen from the schematic in Figure 7, in the case of the Sentinel-2 satellite imagery we are examining both the utility of spectral bands and vegetation indices and the extraction of phenological phases from preselected channels/vegetation indices. These are two seemingly separate parts that will be merged based on the results to provide a more comprehensive overview of the usefulness of Sentinel-2 data for phenological monitoring.

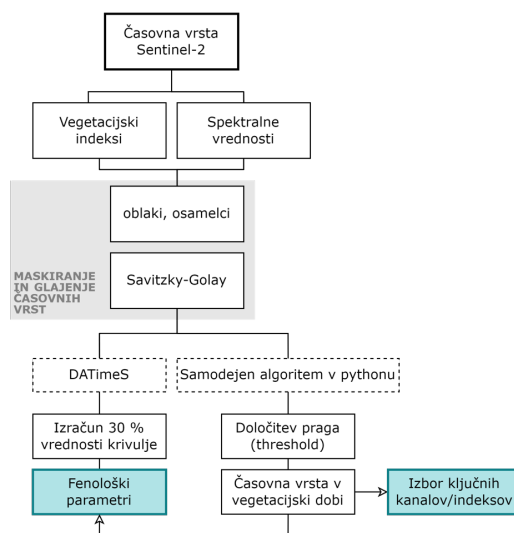


Figure 7. Sentinel-2 satellite image processing workflow for defining phenological phases.

### 4.2.1 Selection of key information for phenology monitoring from Sentinel-2 data

The Sentinel-2 time series are processed and analysed in the open-source Python programming environment (version 3.7.3.), where a number of data processing libraries are available, such as numpy, pandas, matplotlib, seaborn, sentinelhub-py, rasterio, datetime, scipy.signal, etc. There, vegetation indices are first computed from the extracted reflectance values of spectral bands and cloud cover. Then, masking and cleaning of the data is performed, followed by smoothing and temporal interpolation.

The time series are masked with a measure of cloud cover ( $> 0.15\%$ ) to exclude unusable data that are potentially covered by clouds (see Figure 8). The cloud masking threshold is determined experimentally.

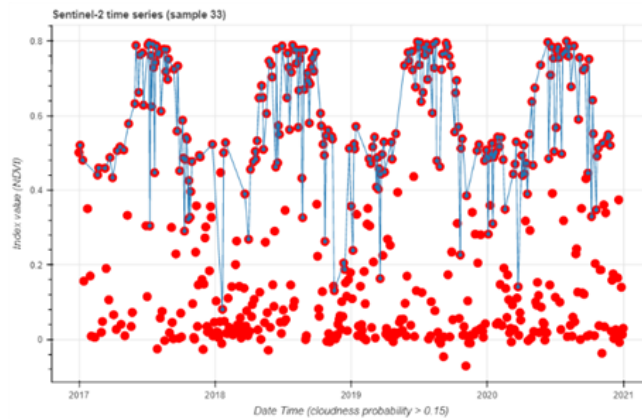


Figure 8. Cloud masking in the time series. The red dots represent all measurements at the location, the blue line includes only the masked values.

In time series, we check for breaks that are not expected, i.e., sudden drops/jumps immediately followed by a sharp rise/fall. Such values are called outliers and are removed from the time series (see Figure 9). The removal of outliers was developed by Löw and Koukal, 2020. The criterion for removing outliers is to remove from the time series all values where the difference in NDVI vegetation index is greater than or less than 0.33 and the time interval between consecutive observation days is less than 90 days.

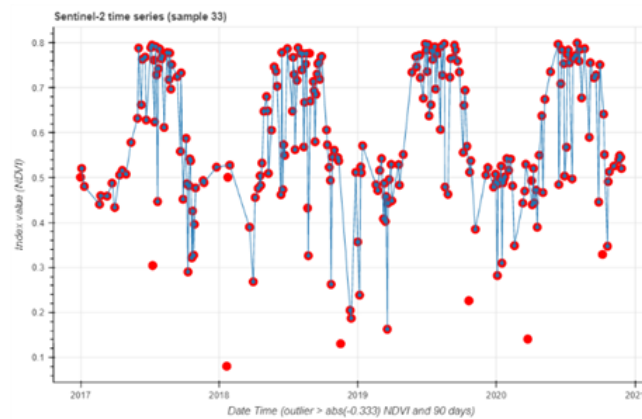


Figure 9. Clearing isolates from the time series.

In the Savitzky-Golay method, the trends and the details of the upward and downward movements of the values are preserved, but no adjustment is made for each individual measurement. We use a window of dimension 31 and a polynomial of degree 3. We fill in the temporal gaps caused by clouds and isolate the clearing using the linear interpolation method and fit the time series to the temporal interval between each observation, in our case 5 days. The resulting time series (Figure 10) is the input for parameter analysis and the determination of phenological metrics using DATimeS.

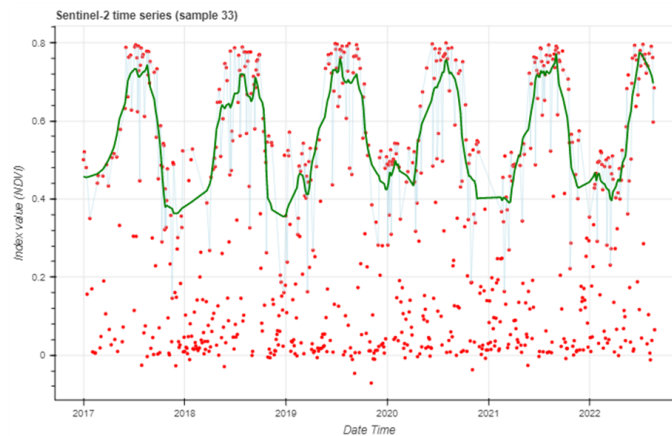


Figure 10. Time series (green line) created to analyse the usefulness of spectral bands in comparison with vegetation indices and phenological parameters coverage.

The time series include meteorological data, namely minimum/maximum and average daily temperature, precipitation, hours of sunshine, and snow cover. As is known from many studies (D’Odorico et al., 2015; Moon et al., 2021; Zhao et al., 2020), meteorological data have a decisive influence on phenological phenomena, so phenological metrics can be predicted from meteorological data alone using so-called agrometeorological models. It logically follows that phenological metrics can be correctly predicted from any time series of satellite imagery linearly linked to meteorological data.

By calculating the correlation matrix (values of Pearson coefficient), we evaluate the utility of all Sentinel-2 spectral bands (B01 - B12), the 22 vegetation indices, and the meteorological data for detecting the growing season and phenological phases. All spectral channels and vegetation indices that are found to be unsuitable are removed from the analysis. The vegetation indices that proved to be most useful for our purposes are used to determine the phenological phases with the DATimeS tool.

#### 4.2.2 DATimeS, version 1.10

DATimeS is a time series decomposition and analysis software developed in MATLAB (Belda et al., 2020). DATimeS allows performing a number of tasks related to time series, such as creating gapless linked spatio-temporal data (images) using machine learning methods (e.g., Gaussian Process Regression - GPR), merging multiple sensor data, and determining phenological phases in multi-year time series. The difference between DATimeS and the previously presented TIMESAT is that DATimeS offers sophisticated new machine learning techniques in addition to the usual methods and tools for time series processing.

Input can be in the form of satellite imagery or a single time series in the form of a text .txt file. This is a time-consuming process, as each time series must be prepared and processed separately to obtain the final estimates of the phenological phases.

DATimeS determines the number of observed growing seasons by calculating the amplitude, the difference between the maximum value in the annual time series and the minimum value, separately for spring and fall, and seasonally decomposing the time series (seasonal decomposition). After the decomposition of the time series, each individual growing season is analysed, and the phenological parameters of the start of the growing season (SOS), end of the growing season (EOS), length of the

season, maximum value in the season, etc. are determined. For the detection of the phenological phases, DATimeS has implemented three different methods: (1) seasonal, (2) relative, and (3) absolute amplitude. In the first case, which is also used here, SOS/EOS is identified where the left/right part of the curve reaches a fraction of the seasonal amplitude (30%) along the rising/falling part of the curve (Figure 11).

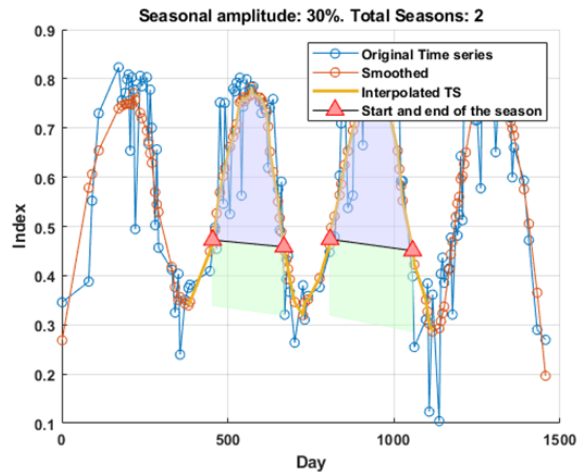


Figure 11. Example of phenological parameter detection with DATimeS. The purple and green colours indicate the areas under the SOS/EOS curve (red triangles) and the spring/fall minimum value, respectively.

## 5 Overview of results

In this section, we present all the results obtained in this study accordingly.

### 5.1 Linking meteorological data with Sentinel-2 time series and selection of products illustrating phenology

Figure 12 shows that the time series of vegetation indices (e.g., NDVI) and reflectance values of spectral band B8A indicate four annual growing seasons between 2017 and 2021, as do the meteorological time series (e.g., mean and minimum temperature). This indicates that the data are correlated/correlated.

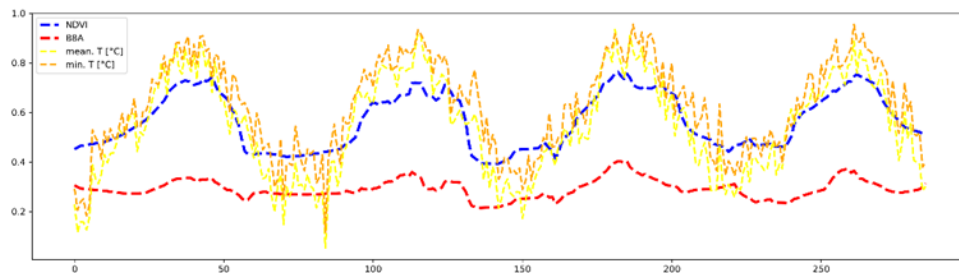
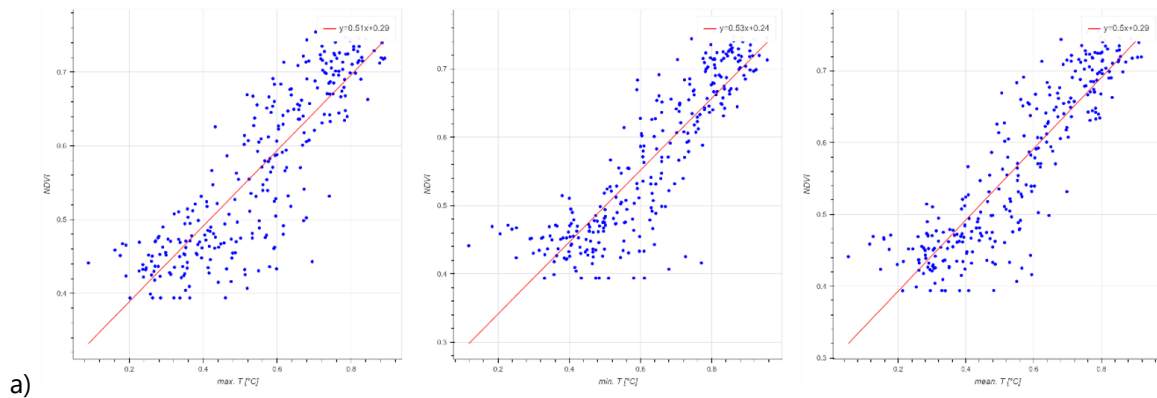


Figure 12. Time series of the selected vegetation index NDVI (blue line), values of spectral band 8A (red line), and minimum and average daily temperatures (orange and yellow lines).

For the correlation analysis, we selected two sites in climatically different parts of Slovenia, namely Rateče (Figure 13, a) in the northwest and Maribor (Figure 13, b) in the east. Both sites showed a high linear relationship between temperature and vegetation NDVI. The highest correlation between the data is obtained in the case of linear relationship between daily minimum temperature and NDVI.



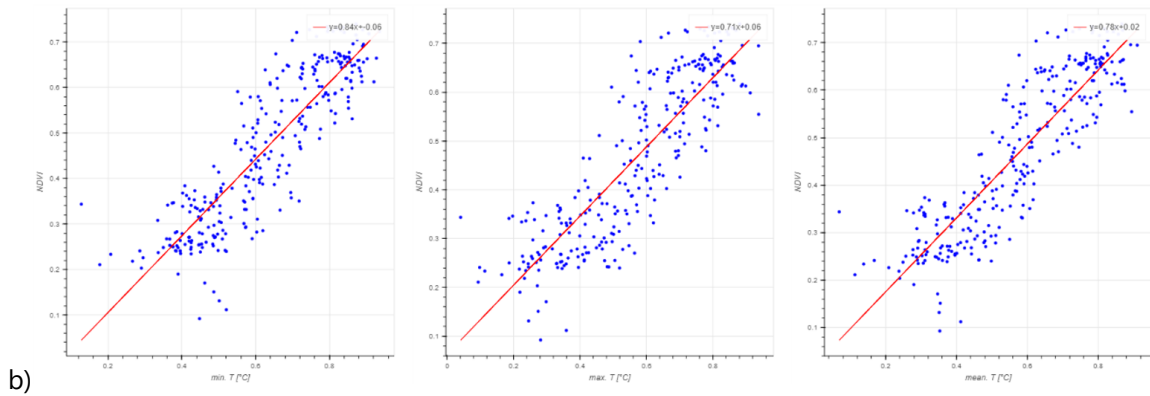


Figure 13. Linear relationship between mean (left), minimum (centre), and maximum (right) temperature and NDVI vegetation index.

The correlation matrix in Figure 14 shows a linear relationship between the vegetation index time series, the Sentinel-2 spectral bands, and the meteorological data. The strong linear correlation, represented by the red colour, indicates that the data are suitable for determining phenological phases. We note that the meteorological data on temperature and number of sunshine hours are important for the recognition of phenology of beech. Spectral bands B06 and B07 (red edge) and bands B08 and B8A (near infrared) are important. Red edge is the abrupt change in reflectance in the range of  $680 \pm 740$  nm. The abrupt change is due to a combination of strong chlorophyll absorption and internal scattering by the leaves. The red edge, the point where red absorption transitions to the near infrared, contains information about chlorophyll content, nitrogen content, and growth status.

The vegetation indices NDVI, TNDVI, GNDVI2, PSSRa, RVI, ARVI, BWDRVI, SAVI, EVI, EVI2, DSWI, GCI, GNDVI, IRECI, SIPI, NBR, MCARI, RGVI, BNIR, NDI45, S2REP and NDMI are important.

The NDVI, SAVI, EVI2, IRECI, BWDRVI, and S2REP indices were found to be the most appropriate (highest linear correlation with field data). NDVI is the most commonly used index in vegetation studies. SAVI is one of the indices that reduce the influence of ground brightness (ground noise) on spectral vegetation indices, which include red and near-infrared (NIR) wavelengths.

IRECI and S2REP are indices with red-edge wavelengths. In particular, S2REP is sensitive to vegetation condition (chlorophyll content) N and growth. In general, the higher the S2REP value, the higher the chlorophyll content. IRECI includes reflectance in four bands to estimate canopy chlorophyll content (Frampton et al., 2013).

The latter are used for a detailed analysis of the detection of phenological phases with DATimeS.

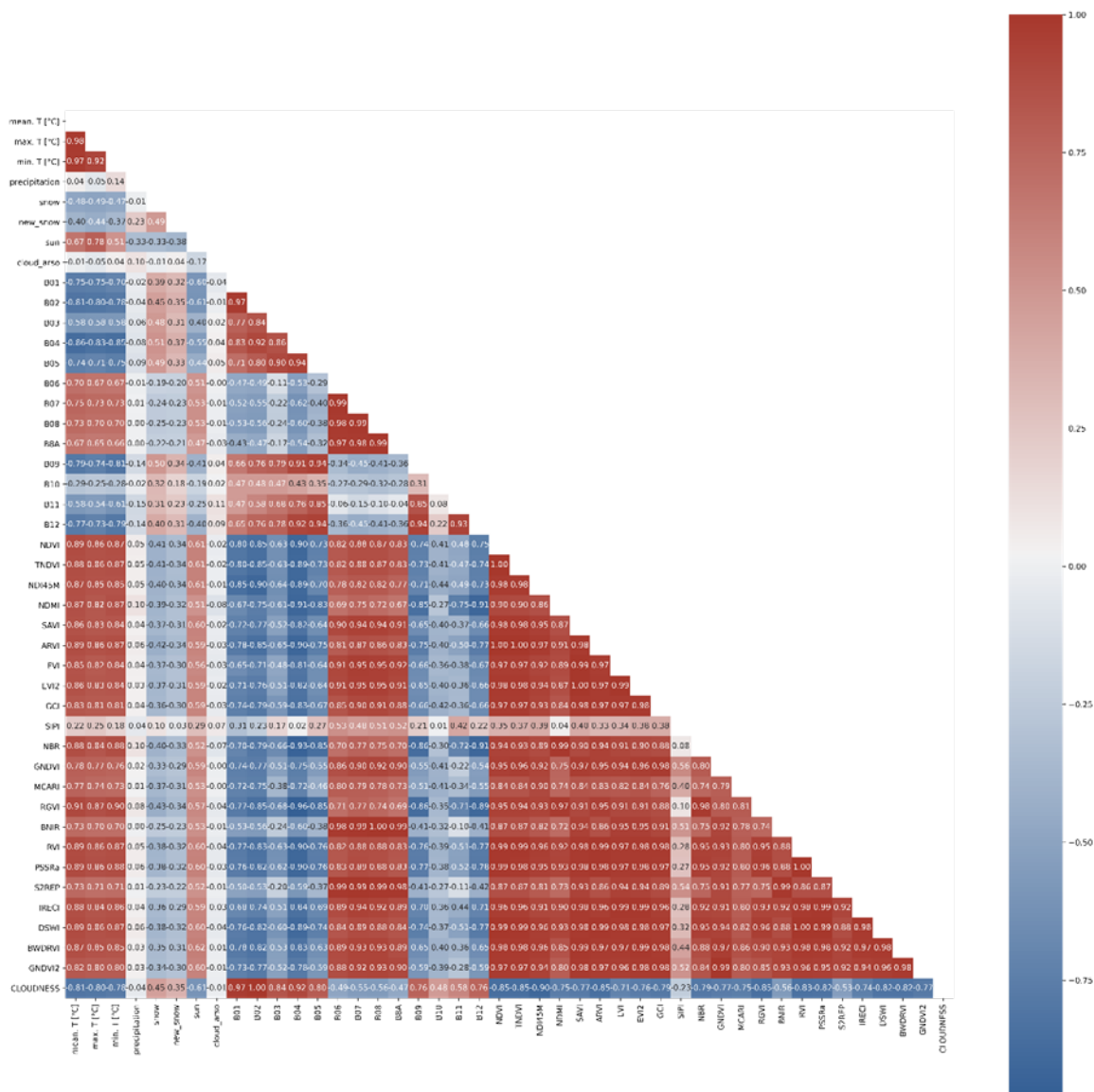


Figure 14. Correlation matrix of time series used (meteorological data, Sentinel-2 spectral channels, and vegetation indices). Red values of the Pearson coefficient indicate that the data are strongly linearly correlated.

## 5.2 Detection of phenological phases from Sentinel-2 data

Comparison of field measurements (in-situ) and phenological parameters from time series of different vegetation indices (Figure 15) shows that the start of the growing season is detected by satellite imagery on average 2-3 weeks earlier than the observer records it in the field. The end of the growing season is detected on average two weeks later by satellite imagery than by field observations. This means that the phenological data obtained from satellite imagery cannot be directly compared in absolute terms with the data obtained in the field, since we are obviously observing and comparing different vegetation phenomena.

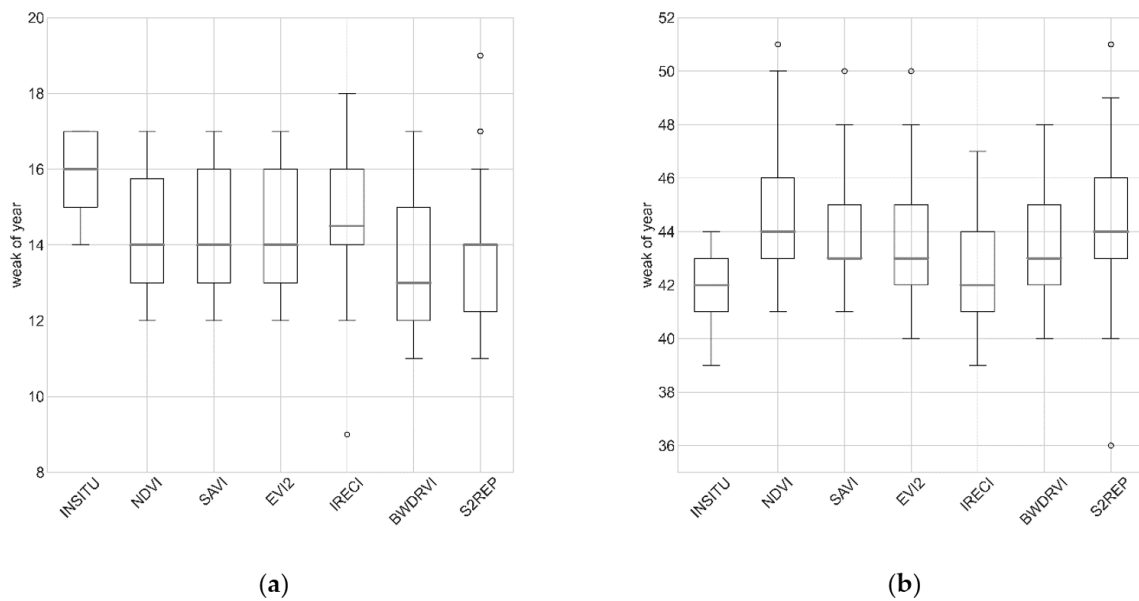


Figure 15. Detection of the beginning (a) and the end of the growing season (b) in all analysed study areas between 2018 and 2021.

In absolute terms, the linear relationship between field-collected phenological data and satellite imagery data is weak (Figure 16). The correlation coefficient for the start of the growing season is 0.38, while the value for the detection of the end of the season increases to 0.45, but still does not show a statistically significant pattern between the data.

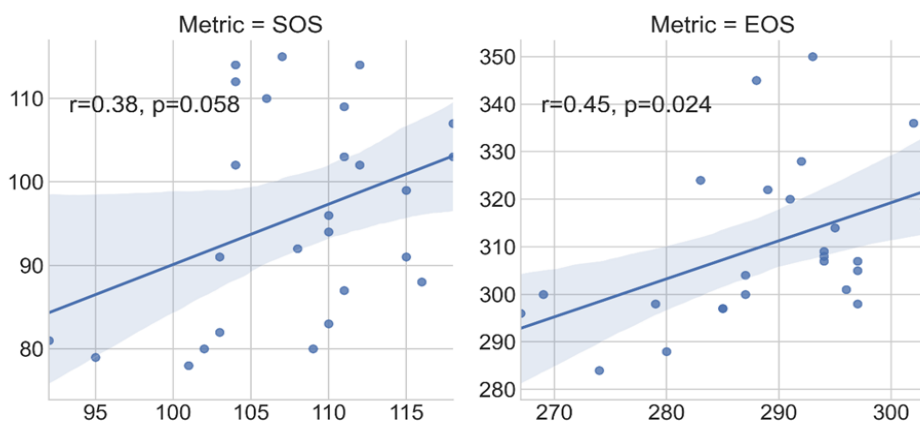


Figure 16. The scatter plot shows the correlation (Pearson coefficient) between the phenological phases of the SOS (left) and the EOS (right) with in-situ soil measurements (x-axis) and phenological phases derived from the NDVI time series (y-axis). Both figures use DOY values and measurements from all analysed study sites during 2017-2021.

Since we cannot achieve absolute correlation of the results, we want to check the relative correlation of the phenological phases at two locations (Rateče, Maribor), which are located in climatically different parts of Slovenia. Figure 17 shows the values of NDVI indices between 2018 and 2021, marking the start and end of vegetation periods. It can be observed that the growing season of beech in the Maribor region starts 2-3 weeks earlier than in Rateče. The end of the beech growing season is 2-3 weeks longer

in the Maribor region than in Rateče. The same results can be seen from the field data (see Table 3), which means that the phenological data obtained from the Sentinel-2 time series compare relatively well with the phenological data collected in the field.

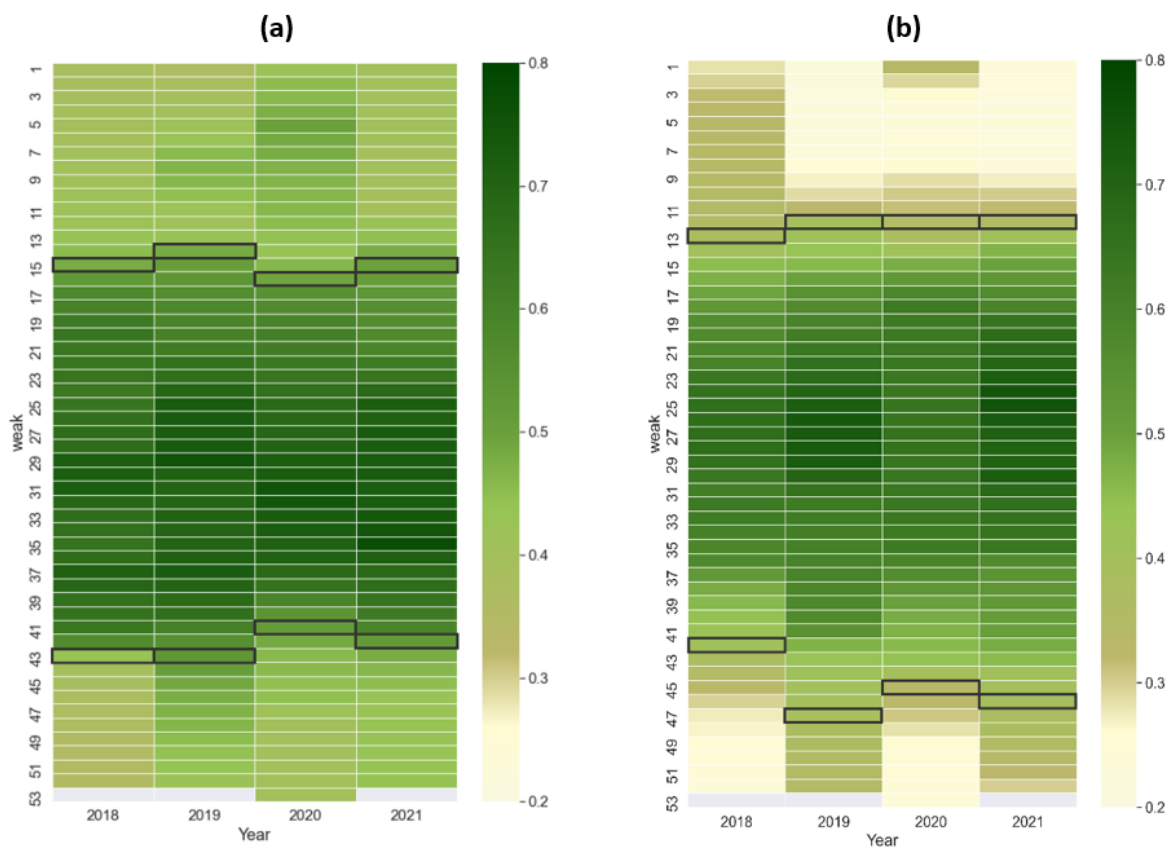


Figure 17. Collection of phenological phases with time series NDVI in the area of Rateče (a) and Maribor (b).

Table 3. Start and end of growing seasons (corresponding to one week of the year) according to phenological data collected in the field (in-situ).

Postaja	Faza	Leto	NDVI	S2REP	BWDRVI	IRECI	EVI2	SAVI	in-situ
Rateče	SOS	2018	15	16	15	16	16	16	17
		2019	14	12	13	16	14	14	16
		2020	16	19	17	18	17	17	17
		2021	15	17	16	19	17	17	/
	EOS	2018	43	43	43	42	42	43	39
		2019	43	40	42	41	42	42	41
		2020	41	42	40	40	40	41	40
		2021	42	41	42	41	42	42	/
		2018	13	14	12	9	12	12	15

<b>Maribor</b>	SOS	2019	12	12	12	13	12	12	14
		2020	12	11	12	14	13	13	14
		2021	12	12	12	13	13	13	/
	EOS	2018	44	44	43	42	43	43	41
		2019	47	45	43	43	43	43	42
		2020	45	45	44	44	45	45	43
		2021	46	43	43	43	43	43	/

### 5.3 Comparison of field data with MODIS-derived phenological phases

The beginning and end of the growing season are expected to vary by a few days from year to year, which may be due to precipitation patterns and atmospheric circulation (Broich et al., 2014). In Table 4, we compare the mean values determined for all years for: 1.) the start of the growing season (SOS), 2.) the end of the growing season (EOS) and 3.) the length of the growing season (LGS) for all points, calculated from MODIS satellite imagery using the seasonal midpoint (SM) method, with field data (phenological, forestry, and meteorological).

*Table 4. Start and end of growing seasons (equal to specific day of the year) and length of growing seasons (total number of days) according to ARSO phenological (\_pheno), GIS phenological (\_forest), and meteorological (\_meteo) field data, compared with data derived from MODIS satellite imagery and determined by the SM method.*

<b>ARSO pheno</b>	<b>SOS_pheno</b>	<b>SOS_SM</b>	<b>EOS_pheno</b>	<b>EOS_SM</b>	<b>LGS_pheno</b>	<b>LGS_SM</b>
Bukovci	111	138	269	307	158	169
Portorož	100	117	303	297	203	180
Boh. Češnjica	119	123	277	303	157	180
Vrhnika	109	101	273	276	164	174
Luče	110	127	274	305	163	178
Šmartno pri SG	110	137	289	318	179	180
Zg. Jezersko	126	120	272	299	146	179
<b>GIS pheno</b>	<b>SOS_forest</b>	<b>SOS_SM</b>	<b>EOS_forest</b>	<b>EOS_SM</b>	<b>LGS_forest</b>	<b>LGS_SM</b>
Point 2	112	116	302	299	190	183
Point 5	113	127	290	307	176	180
Point 7	115	124	293	302	178	178
Point 8	120	119	283	297	163	178

Point 9	115	133	286	317	171	184
Point 10	101	100	297	284	196	184
Point 11	102	103	309	288	207	185
<b>ARSO meteo</b>	<b>SOS_meteo</b>	<b>SOS_SM</b>	<b>EOS_meteo</b>	<b>EOS_SM</b>	<b>LGS_meteo</b>	<b>LGS_SM</b>
Ljubljana	68	98	330	278	262	180
Bilje	54	129	339	311	285	182
Novo Mesto	69	110	322	293	253	183
M. Sobota	73	109	325	299	252	190
Rateče	99	140	307	322	208	182
Vipava	57	112	344	312	287	200
Maribor	70	109	325	295	254	186

A clear pattern can be seen in ARSO and Forest phenological field data in most regions: the start of the growing season is between May and June, and the end of the growing season is in September and October. Meteorological data show an earlier start of the season in March and April and a later end of the season in October and November, resulting in an overall longer meteorological season.

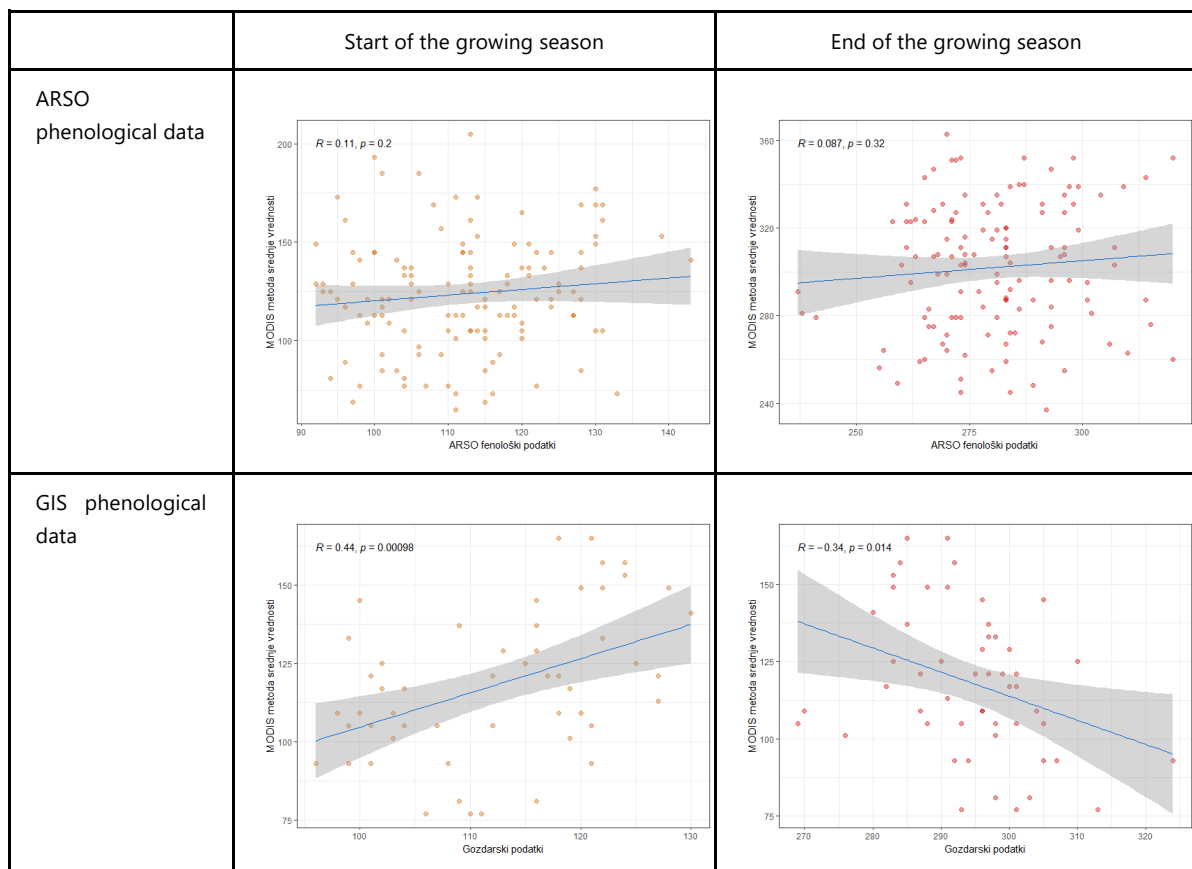
The Table 4 shows that the determination of phenological phases using satellite imagery is the most appropriate compared to forestry phenological data, with minimal deviation in some cases (points 8, 10, and 11: the difference between the start of the growing season is only one day), and the absolute differences for forestry data are also the smallest compared to all field data reviewed (average of 8 days for SOS, 15 days for EOS, and 10 days for LGS). In contrast, comparisons of satellite and meteorological phenology data generally proved to be less accurate. Some measured stations have larger absolute errors, with the largest differences reaching as much as a 75-day difference at the beginning of the growing season (Bilje station) and even larger differences in the length of the growing season (the absolute difference between the two measurements averages about 70 days). However, the phenological data from ARSO are somewhere between the forestry and meteorological observations, reaching a difference from the MODIS measurements of 15 days on average for SOS and 23 days for EOS. For growing season length, the data differ by an average of 16 days.

Pearson correlation was used to calculate the correlation of phenological phases between the satellite images and the three types of field data. First, we calculated the correlation between the start and end of the growing season between MODIS data obtained from the NDVI time series using the seasonal mean approach and the different types of field data (Table 5). The correlation between the variables proved to be a weak but statistically significant. A medium or moderate correlation between the variables is found only for the forestry data, where the correlation coefficient for the SOS is 0.44, while for these data there is a low or weak negative correlation (-0.27) for the EOS.

Table 5. Pearson correlation between phenological, forestry, and meteorological data compared to the method of seasonal midpoint method applied to MODIS NDVI time series.

	Start of the growing season		End of the growing season	
	p-value	Corr. coefficient (R)	p-value	Corr. coefficient (R)
ARSO phenological data	0.20	0.11	0.32	0.087
GIS phenological data	0.001	0.44	0.05	-0.27
ARSO meteorological data	0.021	0.23	0.61	0.05

The scatter plot of SOS and EOS for all pixels and for all years considered is shown in the Figure 18 below. When the data are compared with forestry field data, there is a slope of the curve indicating a (positive or negative) correlation.



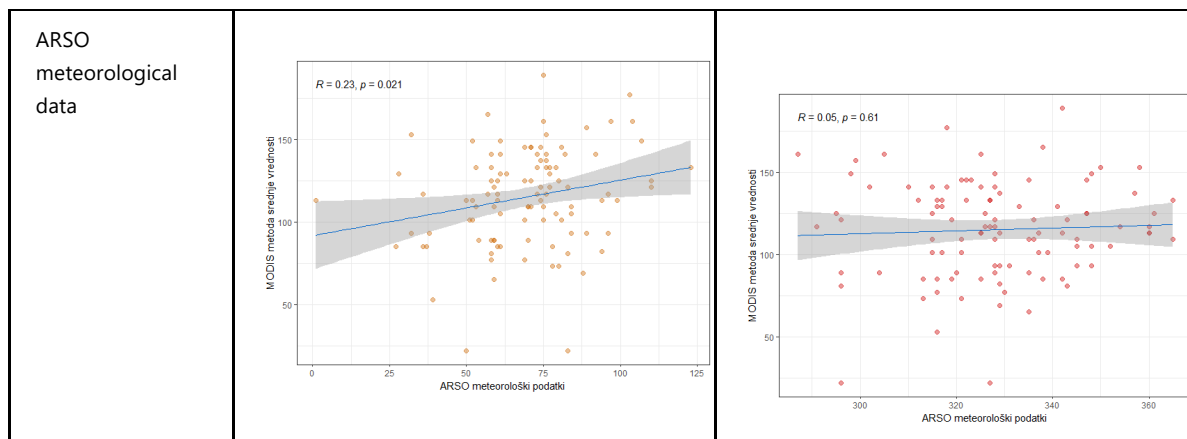


Figure 18. Scatter plots of various field data compared with satellite-based data SOS and EOS.

## 5.4 Comparison of the different approaches for the detection of phenological phases

We compared the results of the determined phenological phases using different methods: the seasonal midpoint method and three different approaches integrated into the TIMESAT algorithm, focusing on the differences with the field data. This was done to rule out misinterpretation of results due to errors in the chosen approach and to test the usefulness of satellite imagery for determining phenological phases. The plots in Figure 19 show the differences between the values of the selected data.

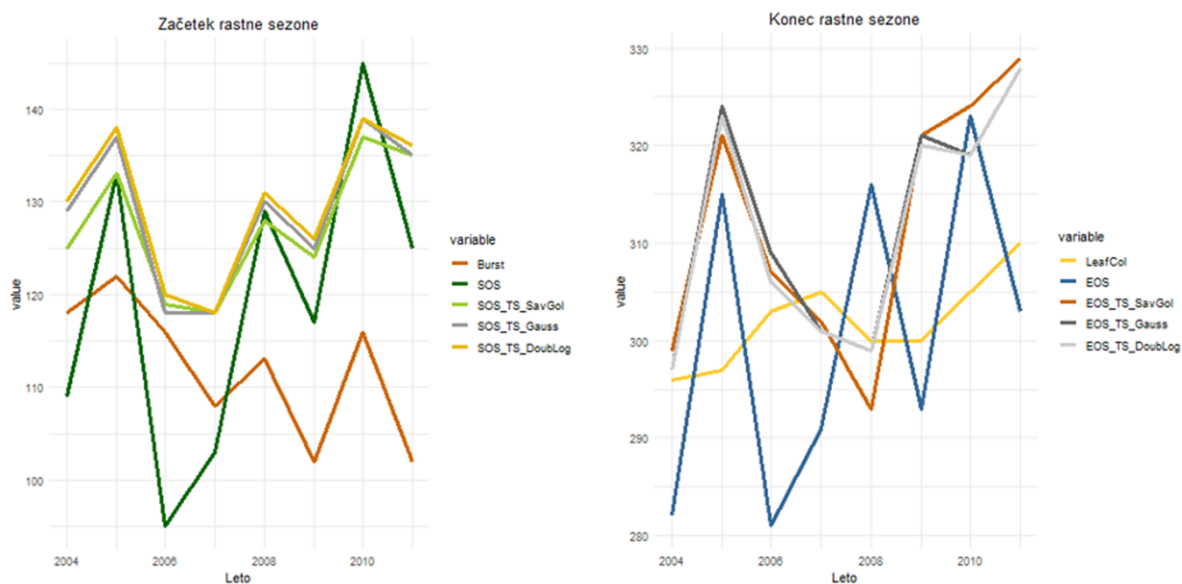


Figure 19. Comparison of the start and end of the growing season at the selected forest phenological point (Burst, LeafCol values) compared to the seasonal midpoint method (SOS, EOS values) and the results of various smoothing runs using the TIMESAT software environment (SOS\_TS and EOS\_TS values). The start and end of the season are given as dates in the calendar year.

As can be seen from the results, there is some variation between the results of the different approaches. On average, the start of the growing season is between 100-140 days (April-May), while the end of the

growing season is between 290-325 days (October-November). Both graphs show that the start of the growing season based on satellite imagery is generally found to be later (by about 15%) than defined by forestry experts, as is the end of the growing season when the different approaches are applied..

We also reviewed the correlation between different methods of determining phenological phases from MODIS satellite imagery with forestry field data and ARSO meteorological data. ARSO phenological data were not compared with other methods in the TIMESAT software tool in this step because these data were not initially available.

*Table 6. Linking the various used methods that we applied to MODIS data with forestry and meteorological data for the beginning and end of the growing season.*

		Start of the growing season		End of the growing season	
		p-value	Corr. coefficient (R)	p-value	Corr. coefficient (R)
GIS phenological data	SM method	0.001	0.44	0.05	-0.27
	TS_SavGol	0.55	-0.085	0.00003	-0.54
	TS_Gauss	0.047	0.28	0.38	-0.12
	TS_DoubLog	0.018	0.35	0.30	0.16
ARSO meteorological data	SM method	0.021	0.23	0.61	0.05
	TS_SavGol	0.1	0.16	0.56	0.059
	TS_Gauss	0.056	0.19	0.21	0.13
	TS_DoubLog	0.05	0.19	0.18	0.13

As can be seen from Table 6 different methods lead to different results. In both cases, the best correlation with the reference field data is the SM method, which in the case of the forest data has a correlation of 0.44 for the SOS and a negative correlation of 0.27 for the EOS. The other TIMESAT methods do not show significant correlation with the field data, but in almost all cases the comparisons are significant, as indicated by p-values of less than 0.05. The results obtained are consistent with the findings of White et al. (2009) and Misra et al. (2016), which indicate that calculated phenological phases can vary widely among different methods for analysing satellite imagery, suggesting that the choice of method for determining phenological phases is critical to obtaining meaningful results.

## 6 Conclusion

The determination of phenological phases is important in several respects. The main advantage of satellite imagery compared to field data is that the determination of phenological parameters is not tied to the type of plant species observed and can be done simultaneously over a large area. Although some authors (e.g., Siłuch et al., 2022) claim that satellite imagery has an advantage over field data in providing vegetation information, we do not believe that this is necessarily true. The problem with comparing calculated phenological parameters from satellite imagery with reference data is that the data are not clearly comparable. For example, the start of the growing season may coincide with the seeding period, where 14 days may be added to the day of the year, or as many as are needed for the plant to visibly green. Similarly, field observations differ, and the start of the growing season is defined differently for phenological observations (GIS, ARSO) or meteorological observations (ARSO). Thus, from the examples described above, it is clear that there is a great deal of variability in the definition of the phenological phases themselves. When modelling phenology, care should be taken to ensure that the area of the observed pixel represents the phenology of the land surface or mixed vegetation in the area under consideration, and not necessarily any particular vegetation unless it occupies the entire area of the pixel. In addition, the modelling often does not take into account elevation, slope, and exposure, which have a visible influence on the phenological characteristics of the vegetation. At the same time, the end of the growing season is more difficult to determine from remote sensing data than the start of the growing season, and the results are much more heterogeneous than those of the start of the growing season (Piao et al., 2019). As highlighted in the previous section, the problem of choosing an appropriate method for determining seasonal phases from remote sensing data arises (Siłuch et al., 2022).

In our study, forestry data proved to be the best compared to satellite imagery. These field data are measured in forested areas or forest edges and are most comparable to the satellite observations in terms of the type of surrounding land use. This is because satellite imagery not only observes a tree in the field at the point (pixel) level and compares its measurements, but also its entire surrounding area. In fact, the phenology of all tree species present in the pixel area is measured at the pixel level. To obtain meaningful results, one would need to calculate the proportion of vegetation for each pixel in the satellite image based on the points examined.

Phenological data obtained with ARSO are less suitable for low- or medium-resolution satellite observations because individual trees of a given species are observed that are not representative in a single pixel, and consequently, instead of a single species in a pixel, several different species with different phenological behaviour are found. In addition, it should be remembered that phenological field data do not always refer to a specific coordinate, but to an area that is usually within a radius of 1 km, or more in exceptional cases. Erroneous NDVI values can therefore lead to incorrect estimates of the start and end of phenological phases or their estimates. The low resolution of the products of MODIS NDVI (250 m) does not provide the homogeneous pixels needed to account for the large variability in vegetation phenology in the areas considered. This was also noted by Younes et al. (2021), who showed that the resolution of MODIS images is too high to study the phenology of a particular species and that these models cannot accurately describe the phenology of a particular type of vegetation, but they do provide useful clues to the phenology of the area under consideration. Therefore, in order to meaningfully determine phenological phases from coarse resolution data, we should observe monocultures that span a larger area. The higher spatial resolution of satellite imagery, e.g., from Landsat or Sentinel-2 sensors, allows for more accurate matching of time series parameters with data measured

in the field (Fisher et al., 2006; Jönsson et al., 2018; Melaas et al., 2013). Therefore, the increased number of observations with Sentinel-2 imagery, available in dense time series only since 2017, may further increase the accuracy of determining phenological phases (Jönsson et al., 2018).

It should be noted that the ARSO meteorological data are not directly phenological data, the monitoring sites are located in areas where the pixel coverage of vegetation is lower (in urban areas), and consequently the NDVI results cannot reflect the vegetation condition in these areas due to the influence of other land uses. Nevertheless, the comparison is based on the assumption that vegetation development (mainly of deciduous trees) is related to ambient temperatures. These data were therefore used to compare how results obtained from satellite imagery relate to these data.

However, comparison between observed remotely sensed vegetation indices and vegetation productivity values provides valuable insight into the usefulness of remotely sensed vegetation indices for validation, refinement, and general improvement of vegetation simulation.

## 7 References

- Akkartala, A., Türüdüa, O., Erbekb, F.S. (Eds.), 2004. Analysis of changes in vegetation biomass using multitemporal and multisensor satellite data. ISPRS archives.
- Belda, S., Pipia, L., Morcillo-Pallarés, P., Rivera-Caicedo, J.P., Amin, E., Grave, C. de, Verrelst, J., 2020. DATimeS: A machine learning time series GUI toolbox for gap-filling and vegetation phenology trends detection. *Environmental Modelling & Software* 127, 104666. <https://doi.org/10.1016/j.envsoft.2020.104666>.
- Blackburn, G.A., 1998. Quantifying chlorophylls and carotenoids at leaf and canopy scales: An evaluation of some hyperspectral approaches. *Remote Sensing of Environment* 66, 273–285. [https://doi.org/10.1016/S0034-4257\(98\)00059-5](https://doi.org/10.1016/S0034-4257(98)00059-5).
- Bolton, D.K., Gray, J.M., Melaas, E.K., Moon, M., Eklundh, L., Friedl, M.A., 2020. Continental-scale land surface phenology from harmonized Landsat 8 and Sentinel-2 imagery. *Remote Sens. Environ.* 240, 111685. <https://doi.org/10.1016/j.rse.2020.111685>
- Broich, M., Huete, A., Tulbure, M.G., Ma, X., Xin, Q., Paget, M., Restrepo-Coupe, N., Davies, K., Devadas, R., Held, A., 2014. Land surface phenological response to decadal climate variability across Australia using satellite remote sensing. *Biogeosciences* 11, 5181–5198. <https://doi.org/10.5194/bg-11-5181-2014>
- Cai, Z., Jönsson, P., Jin, H., Eklundh, L., 2017. Performance of Smoothing Methods for Reconstructing NDVI Time-Series and Estimating Vegetation Phenology from MODIS Data. *Remote Sens.* 9, 1271. <https://doi.org/10.3390/rs9121271>
- Chen, J., Jönsson, P., Tamura, M., Gu, Z., Matsushita, B., Eklundh, L., 2004. A simple method for reconstructing a high-quality NDVI time-series data set based on the Savitzky–Golay filter. *Remote Sens. Environ.* 91, 332–344. <https://doi.org/10.1016/j.rse.2004.03.014>
- Cho, M.A., Ramoelo, A., Dziba, L., 2017. Response of Land Surface Phenology to Variation in Tree Cover during Green-Up and Senescence Periods in the Semi-Arid Savanna of Southern Africa. *Remote Sens.* 9, 689. <https://doi.org/10.3390/rs9070689>
- Črepinšek, Z., 2002. Napovedovanje fenološkega razvoja rastlin na osnovi agrometeoroloških spremenljivk v Sloveniji: Prediction of Phenological Development of Plants Based on Agrimeteorological Variables in Slovenia. Doctoral Thesis. Univerza v Ljubljani, 157 pp.
- D’Odorico, P., Gonsamo, A., Gough, C.M., Bohrer, G., Morison, J., Wilkinson, M., Hanson, P.J., Gianelle, D., Fuentes, J.D., Buchmann, N., 2015. The match and mismatch between photosynthesis and land surface phenology of deciduous forests. *AGRICULTURAL AND FOREST METEOROLOGY* 214, 25–38. <https://doi.org/10.1016/j.agrformet.2015.07.005>.
- Daughtry, C.S., Walthall, C.L., Kim, M.S., Colstoun, E.B. de, McMurtrey, J.E., 2000. Estimating corn leaf chlorophyll concentration from leaf and canopy reflectance. *Remote Sensing of Environment* 74, 229–239. [https://doi.org/10.1016/S0034-4257\(00\)00113-9](https://doi.org/10.1016/S0034-4257(00)00113-9).
- Davis, C., Hoffman, M., Roberts, W., 2017. Long-term trends in vegetation phenology and productivity over Namaqualand using the GIMMS AVHRR NDVI3g data from 1982 to 2011. <https://doi.org/10.1016/J.SAJB.2017.03.007>
- Delegido, J., Verrelst, J., Alonso, L., Moreno, J., 2011. Evaluation of Sentinel-2 red-edge bands for empirical estimation of green LAI and chlorophyll content. *Sensors (Basel, Switzerland)* 11, 7063–7081. <https://doi.org/10.3390/s110707063>.
- Eklundh, L., Jönsson, P., 2017. TIMESAT 3.3 with seasonal trend decomposition and parallel processing - Software Manual.
- EOS Data Analytics, 2022. Vegetation Indices As A Satellite-Based Add-On For Agri Solutions. <https://eos.com/blog/vegetation-indices/> (accessed 23 December 2022).
- Fisher, J.I., Mustard, J.F., Vadeboncoeur, M.A., 2006. Green leaf phenology at Landsat resolution: Scaling from the field to the satellite. *Remote Sens. Environ.* 100, 265–279. <https://doi.org/10.1016/j.rse.2005.10.022>
- Frampton, W.J., Dash, J., Watmough, G., Milton, E.J., 2013. Evaluating the capabilities of Sentinel-2 for quantitative estimation of biophysical variables in vegetation. *ISPRS Journal of Photogrammetry and Remote Sensing* 82, 83–92. <https://doi.org/10.1016/j.isprsjprs.2013.04.007>.
- Gao, B., 1996. NDWI—A normalized difference water index for remote sensing of vegetation liquid water from space. *Remote Sensing of Environment* 58, 257–266. [https://doi.org/10.1016/S0034-4257\(96\)00067-3](https://doi.org/10.1016/S0034-4257(96)00067-3).
- García, M.L., Caselles, V., 1991. Mapping burns and natural reforestation using thematic Mapper data. *Geocarto International* 6, 31–37. <https://doi.org/10.1080/10106049109354290>.
- Garonna, I., de Jong, R., Schaepman, M.E., 2016. Variability and evolution of global land surface phenology over the past three decades (1982–2012). *Glob. Change Biol.* 22, 1456–1468. <https://doi.org/10.1111/gcb.13168>

- Gitelson, A.A., Kaufman, Y.J., Merzlyak, M.N., 1996. Use of a green channel in remote sensing of global vegetation from EOS-MODIS. *Remote Sensing of Environment* 58, 289–298. [https://doi.org/10.1016/S0034-4257\(96\)00072-7](https://doi.org/10.1016/S0034-4257(96)00072-7).
- Hościło, A. Sentinel-2 data and vegetation indices: EO4GEO Lecture.
- Huang, X., Liu, J., Zhu, W., Atzberger, C., Liu, Q., 2019. The Optimal Threshold and Vegetation Index Time Series for Retrieving Crop Phenology Based on a Modified Dynamic Threshold Method. *Remote Sens.* 11, 2725. <https://doi.org/10.3390/rs11232725>
- Huete, A., 1988. A soil-adjusted vegetation index (SAVI). *Remote Sensing of Environment* 25, 295–309. [https://doi.org/10.1016/0034-4257\(88\)90106-X](https://doi.org/10.1016/0034-4257(88)90106-X).
- Huete, A., 1997. A comparison of vegetation indices over a global set of TM images for EOS-MODIS. *Remote Sensing of Environment* 59, 440–451. [https://doi.org/10.1016/S0034-4257\(96\)00112-5](https://doi.org/10.1016/S0034-4257(96)00112-5).
- Huete, A., Didan, K., van Leeuwen, W., Miura, T., Glenn, E., 2011. MODIS Vegetation Indices, in: Ramachandran, B., Justice, C.O., Abrams, M.J. (Eds.), *Land remote sensing and global environmental change: NASA's Earth observing system and the science of ASTER and MODIS / editors, Bhaskar Ramachandran, Christopher O. Justice, Michael J. Abrams*, vol. 11. Springer, New York, London, pp. 579–602.
- Jönsson, P., Cai, Z., Melaas, E., Friedl, M.A., Eklundh, L., 2018. A Method for Robust Estimation of Vegetation Seasonality from Landsat and Sentinel-2 Time Series Data. *Remote Sens.* 10, 635. <https://doi.org/10.3390/rs10040635>
- Jönsson, P., Eklundh, L., 2004. TIMESAT—a program for analyzing time-series of satellite sensor data. *Comput. Geosci.* 30, 833–845. <https://doi.org/10.1016/j.cageo.2004.05.006>
- Kowalski, K., Senf, C., Hostert, P., Pflugmacher, D., 2020. Characterizing spring phenology of temperate broadleaf forests using Landsat and Sentinel-2 time series. *Int. J. Appl. Earth Obs. Geoinformation* 92, 102172. <https://doi.org/10.1016/j.jag.2020.102172>
- Löw, M., Koukal, T., 2020. Phenology Modelling and Forest Disturbance Mapping with Sentinel-2 Time Series in Austria. *Remote Sensing* 12, 4191. <https://doi.org/10.3390/rs12244191>.
- Lymburner, L., Beggs, P.J., Jacobson, C.R., 2000. Estimation of canopy-average surface-specific leaf area using Landsat TM data. *Photogrammetric Engineering and Remote Sensing* 66, 183–191.
- Melaas, E.K., Friedl, M.A., Zhu, Z., 2013. Detecting interannual variation in deciduous broadleaf forest phenology using Landsat TM/ETM+ data. *Remote Sens. Environ.* 132, 176–185. <https://doi.org/10.1016/j.rse.2013.01.011>
- Melaas, E.K., Sulla-Menashe, D., Friedl, M.A., 2018. Multidecadal Changes and Interannual Variation in Springtime Phenology of North American Temperate and Boreal Deciduous Forests. *Geophys. Res. Lett.* 45, 2679–2687. <https://doi.org/10.1002/2017GL076933>
- Misra, G., Buras, A., Menzel, A., 2016. Effects of Different Methods on the Comparison between Land Surface and Ground Phenology—A Methodological Case Study from South-Western Germany. *Remote Sens.* 8, 753. <https://doi.org/10.3390/rs8090753>
- Moon, M., Seyednasrollah, B., Richardson, A.D., Friedl, M.A., 2021. Using time series of MODIS land surface phenology to model temperature and photoperiod controls on spring greenup in North American deciduous forests. *Remote Sensing of Environment* 260. <https://doi.org/10.1016/j.rse.2021.112466>.
- Nasrallah, A., Baghdadi, N., El Hajj, M., Darwish, T., Belhouchette, H., Faour, G., Darwich, S., Mhaweij, M., 2019. Sentinel-1 Data for Winter Wheat Phenology Monitoring and Mapping. *Remote Sens.* 11, 2228. <https://doi.org/10.3390/rs11192228>
- Noumonvi, K.D., Oblišar, G., Žust, A., Vilhar, U., 2021. Empirical Approach for Modelling Tree Phenology in Mixed Forests Using Remote Sensing. *Remote Sens.* 13, 3015. <https://doi.org/10.3390/rs13153015>
- O'Connor, B., Dwyer, E., Cawkwell, F., Eklundh, L., 2012. Spatio-temporal patterns in vegetation start of season across the island of Ireland using the MERIS Global Vegetation Index. *ISPRS J. Photogramm. Remote Sens.* 68, 79–94. <https://doi.org/10.1016/j.isprsjprs.2012.01.004>
- Pearson, R.L., Miller, L.D., 1972. Remote Mapping of Standing Crop Biomass for Estimation of the Productivity of the Shortgrass Prairie. *Remote Sensing of Environment*, VIII, 1355.
- Pettorelli, N., Vik, J.O., Mysterud, A., Gaillard, J.-M., Tucker, C.J., Stenseth, N.Ch., 2005. Using the satellite-derived NDVI to assess ecological responses to environmental change. *Trends Ecol. Evol.* 20, 503–510. <https://doi.org/10.1016/j.tree.2005.05.011>
- Piao, S., Liu, Q., Chen, A., Janssens, I.A., Fu, Y., Dai, J., Liu, L., Lian, X., Shen, M., Zhu, X., 2019. Plant phenology and global climate change: Current progresses and challenges. *Glob. Change Biol.* 25, 1922–1940. <https://doi.org/10.1111/gcb.14619>
- Raspe, S., Fleck, S., Beuker, E., Bastrup-Birk, A., Preuhsler, T., 2020. Part VI: Phenological Observations. Version 2020-03, in: UNECE ICP Forests Programme Co-Ordinating Centre (Ed.): *Manual on Methods and Criteria for*

- Harmonized Sampling, Assessment, Monitoring and Analysis of the Effects of Air Pollution on Forests. Thünen Institute of Forest Ecosystems, Eberswalde, Germany, p. 14.
- Restrepo-Coupe, N., Huete, A., Davies, K., 2015. Satellite Phenology Validation, in: Held, A., Phinn, S., Soto-Berelov, M., Jones, S. (Eds.), *AusCover Good Practice Guidelines: A Technical Handbook Supporting Calibration and Validation Activities of Remotely Sensed Data Products*. TERN AusCover, p. 340.
- Savitzky, Abraham., Golay, M.J.E., 1964. Smoothing and Differentiation of Data by Simplified Least Squares Procedures. *Anal. Chem.* 36, 1627–1639. <https://doi.org/10.1021/ac60214a047>
- Sonobe, R., Yamaya, Y., Tani, H., Wang, X., Kobayashi, N., Mochizuki, K., 2018. Crop classification from Sentinel-2-derived vegetation indices using ensemble learning. *J. Appl. Rem. Sens.* 12, 1. <https://doi.org/10.1117/1.JRS.12.026019>.
- Siłuch, M., Bartmiński, P., Zglobicki, W., 2022. Remote Sensing in Studies of the Growing Season: A Bibliometric Analysis. *Remote Sens.* 14, 1331. <https://doi.org/10.3390/rs14061331>
- Sjöström, M., Ardö, J., Arneeth, A., Boulain, N., Cappelaere, B., Eklundh, L., de Grandcourt, A., Kutsch, W.L., Merbold, L., Nouvellon, Y., Scholes, R.J., Schubert, P., Seaquist, J., Veenendaal, E.M., 2011. Exploring the potential of MODIS EVI for modeling gross primary production across African ecosystems. *Remote Sens. Environ.* 115, 1081–1089. <https://doi.org/10.1016/j.rse.2010.12.013>
- Tanre, D., Holben, B.N., Kaufman, Y.J., 1992. Atmospheric correction algorithm for NOAA-AVHRR products: theory and application. *IEEE Trans. Geosci. Remote Sensing* 30, 231–248. <https://doi.org/10.1109/36.134074>.
- Tucker, C.J., 1979. Red and photographic infrared linear combinations for monitoring vegetation. *Remote Sens. Environ.* 8, 127–150. [https://doi.org/10.1016/0034-4257\(79\)90013-0](https://doi.org/10.1016/0034-4257(79)90013-0)
- Van Leeuwen, W.J.D., 2008. Monitoring the Effects of Forest Restoration Treatments on Post-Fire Vegetation Recovery with MODIS Multitemporal Data. *Sensors* 8, 2017–2042. <https://doi.org/10.3390/s8032017>
- Vrieling, A., Meroni, M., Darvishzadeh, R., Skidmore, A.K., Wang, T., Zurita-Milla, R., Oosterbeek, K., O'Connor, B., Paganini, M., 2018. Vegetation phenology from Sentinel-2 and field cameras for a Dutch barrier island. *Remote Sens. Environ.* 215, 517–529. <https://doi.org/10.1016/j.rse.2018.03.014>
- Wessels, K., Steenkamp, K., von Maltitz, G., Archibald, S., 2011. Remotely sensed vegetation phenology for describing and predicting the biomes of South Africa. *Appl. Veg. Sci.* 14, 49–66. <https://doi.org/10.1111/j.1654-109X.2010.01100.x>
- White, M.A., De BEURS, K.M., Didan, K., Inouye, D.W., Richardson, A.D., Jensen, O.P., O'keefe, J., Zhang, G., Nemani, R.R., Van LEEUWEN, W.J.D., Brown, J.F., De WIT, A., Schaepman, M., Lin, X., Dettinger, M., Bailey, A.S., Kimball, J., Schwartz, M.D., Baldocchi, D.D., Lee, J.T., Lauenroth, W.K., 2009. Intercomparison, interpretation, and assessment of spring phenology in North America estimated from remote sensing for 1982–2006. *Glob. Change Biol.* 15, 2335–2359. <https://doi.org/10.1111/j.1365-2486.2009.01910.x>
- Younes, N., Joyce, K.E., Maier, S.W., 2021. All models of satellite-derived phenology are wrong, but some are useful: A case study from northern Australia. *Int. J. Appl. Earth Obs. Geoinformation* 97, 102285. <https://doi.org/10.1016/j.jag.2020.102285>
- Zhang, X., Friedl, M.A., Schaaf, C.B., Strahler, A.H., Hodges, J.C.F., Gao, F., Reed, B.C., Huete, A., 2003. Monitoring vegetation phenology using MODIS. *Remote Sens. Environ.* 84, 471–475. [https://doi.org/10.1016/S0034-4257\(02\)00135-9](https://doi.org/10.1016/S0034-4257(02)00135-9)
- Zhao, B., Donnelly, A., Schwartz, M.D., 2020. Evaluating autumn phenology derived from field observations, satellite data, and carbon flux measurements in a northern mixed forest, USA. *INTERNATIONAL JOURNAL OF BIOMETEOROLOGY* 64, 713–727. <https://doi.org/10.1007/s00484-020-01861-9>
- Žust, A., Dolinar, M., Sušnik, A., Bergant, K., 2016. Fenologija v Sloveniji: priročnik za fenološka opazovanja: ob 65. letnici delovanja državne fenološke mreže. Ministrstvo za okolje in prostor, Agencija RS za okolje, Ljubljana.